Neilsen, E.A., Waitt, R.B. and Malone, S.D., 1989, Eyewitness accounts and photographs of the 18 May 1980 eruption of Mount St. Helens, Wash., *in* Continental Magmatism, Abstracts, IAVCEI General Assembly, Santa Fe, New Mexico, June 25-July 1: New Mexico Bureau of Mines & Mineral Resources, Bulletin 131, p. 203.

Peterson, D.W., 1986, Mount St. Helens and the science of volcanology: a five-year perspective, *in* Keller, S.A.C., ed., Mount St. Helens: Five Years Later: Eastern Washington University Press, Cheney, WA, p. 3-19.

Rosenbaum, J.G. and Waitt, R.B., Jr., 1981, Summary of eyewitness accounts of the May 18 eruption, *in* Lipman, P.W. and Mullineaux, D.R., eds., The 1980 eruptions of Mount St. Helens, Washington: United States Geological Survey, Professional Paper 1250, p. 53-67.

Sparks, R.S.J., Moore, J.G. and Rice C.J., 1986, The initial giant umbrella cloud of the May 18th, 1980, explosive eruption of Mount St. Helens: Journal of Volcanology and Geothermal Research, v. 28, p. 257-274.

Valentine, G.A., 1987, Stratified flow in pyroclastic surges: Bulletin of Volcanology, v. 49, p. 616-630.

Voight, B., 1981, Time scale for the first moments of the May 18 eruption, *in* Lipman, P.W. and Mullineaux, D.R., eds., The 1980 eruptions of Mount St. Helens, Washington: United States Geological Survey, Professional Paper 1250, p. 69-86.

Waitt, R.B., Jr., 1981, Devastating pyroclastic density flow and attendant air fall of May 18 — stratigraphy and sedimentology of deposits, *in* Lipman, P.W. and Mullineaux, D.R., eds., The 1980 eruptions of Mount St. Helens, Washington: United States Geological Survey, Professional Paper 1250, p. 439-458.

Waitt, R.B., Jr., 1984, Comment and Reply on "Mount St. Helens 1980 and Mount Pelée 1902 — Flow or surge?": Geology, v. 12, p. 693.

Walker, G.P.L. and McBroome, L.A., 1983, Mount St. Helens 1980 and Mount Pelée 1902 — Flow or surge?: Geology, v. 11, p. 571-574.

Walker, G.P.L. and Morgan, L.A., 1984, Comment and Reply on "Mount St. Helens 1980 and Mount Pelee 1902 — Flow or Surge?": Geology, v. 12, p. 693-695.

Compositional Trends and Eruptive Cycles at Mount St. Helens

Clifford A. Hopson
Department of Geological Sciences
University of California
Santa Barbara, CA 93106

William G. Melson
Department of Mineral Sciences
Smithsonian Institution
Washington, DC 20560

Summary
The 40,000-year eruptive history of Mount St. Helens reveals an overall compositional trend from rhyodacite to andesite, with basalt at ~1.9 and ~1.6 ka. A cyclic eruption pattern is superimposed on this trend. Cycles comprised a repose interval, when compositional and thermal gradients developed in the underlying magma body, followed by an eruption interval in which progressive tapping of magma beheaded these gradients. Recovery of gradients varied with duration of the ensuing repose period. Eruption sequences follow the pattern: (1) ***eruptive progression*** from Plinian eruptions to dome growth accompanied by pyroclastic flows and tephra, followed (in some cases) by lava flows punctuated by pyroclastic outbursts; (2) a ***mineralogic progression*** from hydrous Fe-Mg phenocrysts (hb, cm, bi) toward pyroxenes; (3) a ***magmatic compositional progression*** from rhyodacite or dacite to andesite. Progressions 1 and 2 stem mainly from volatile gradients in the magma reservoir whereas progression 3 (and to some extent 2) reflects gradients of melt composition and crystal content. Three eruption cycles within the last 4,000 years follow this pattern. Earlier cycles are probable but only dimly perceived, mainly from the partial record of tephras and pyroclastic flows.

Introduction
This paper stems from a talk given at the GAC—MAC Special Symposium on the Tenth Anniversary of the May 18, 1980, eruption of Mount St. Helens (MSH). Our assignment was to present an overview of some aspect of the eruptive history of MSH prior to 1980. The eruptive history itself has already been established and is now well known. Little has been said as yet, however, about pre-1980 compositional variation of the MSH magmas with time, which is important petrogenetically. We therefore chose to look at compositional trends and eruptive patterns over the lifetime of the MSH volcanic center, and to suggest some possible interpretations. Perhaps this will help to stimulate much-needed future work on these problems.

Eruptive History of Mount St. Helens
The eruptive history of MSH has been established primarily by Dwight R. Crandell and Donal R. Mullineaux. Their detailed, elegant work sets the standard for such studies everywhere.

The eruptive history of the MSH volcanic center spans >40,000 years; that of the present mountain, about 3,000 years (Crandell *et al.*, 1975; Crandell and Mullineaux, 1978; Mullineaux and Crandell, 1981; Crandell, 1987). Crandell (1987) divides the eruptive history of MSH into four ***eruptive stages***, **each separated by long intervals of dormancy: the Ape Canyon stage, >40-36 ka; the Cougar stage, ~21-18 ka; the Swift Creek stage, 13-11 ka, and the Spirit Lake stage,** 4 ka to present. Shorter ***eruptive periods***, separated by repose periods, are recognized within the Spirit Lake eruptive stage. These are: the Smith Creek period, 4.0-3.3 ka; the Pine Creek period, 3.0-2.5 ka; the Castle Creek period, 2.2-1.6 ka; the Sugar Bowl period, 1.15 ka; the Kalama period, ~500-370 years B.P.; the Goat Rocks period, 190-133 years B.P.; and the eruptions that began in 1980. Figure 1 shows the eruptive stages and periods and the dormant intervals that separate them.

The first three eruptive stages and early part of the fourth stage (Smith Creek and Pine Creek periods) produced abundant dacitic tephras and pyroclastic flows (Mullineaux, 1986; Crandell, 1987). Dacitic (to siliceous andesite) dome and lava flow remnants related to these pyroclastics probably lie buried beneath the modern volcano, judging from a few exposed remnants and from the common occurrence of pyroclastic flows bearing nonvesicular clasts of dacitic dome lavas. Remnants of a cluster of dacitic domes mostly from the Pine Creek period are exposed in the lower part of the 1980 crater wall of MSH (Hopson and Melson, 1982). The modern stratovolcano, built mainly from lavas (flows and domes) and pyroclastic deposits of andesite, dacite, and lesser basalt, grew above the pedestal of earlier dome remnants during Castle Creek and later time.

The eruption of olivine basalt during the Castle Creek eruptive period is a unique event in the history of MSH, and it figures prominently in hypotheses concerning the petrogenetic evolution of the volcano. Two basaltic events at ~1.9 ka (Greeley and Hyde,

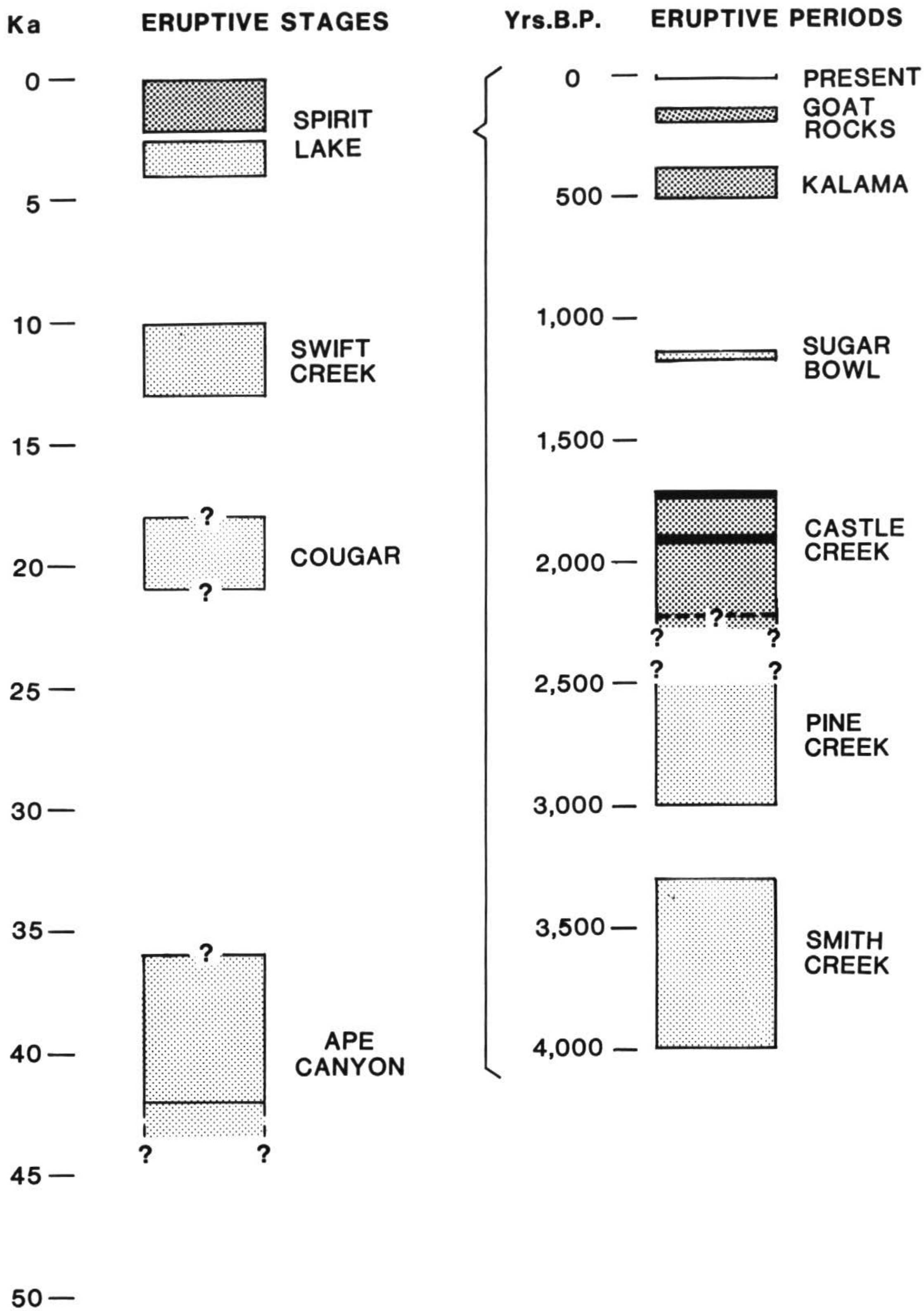

Figure 1 *Eruptive history of Mount St. Helens volcanic center. Left column shows* ***eruptive stages*** *with intervening dormant intervals, from the earliest recognized activity to the present. Right column shows* ***eruptive periods*** *and dormant intervals within the Spirit Lake eruptive stage, ~4,000 years ago to the present. Light stipple depicts chiefly dacitic volcanism; dark stipple indicates andesitic to dacitic volcanism; black bands depict basalt. Terminology and age spans of eruptive stages and periods taken (with minor modification) from Crandell (1987).*

1972) and ~1.7 ka (Mullineaux and Crandell, 1981) have been recognized in the past, but Crandell (1987) now infers only a single basaltic event at ~1.6(?) ka. We believe, however, that the voluminous, compositionally uniform and relatively primitive Cave Basalt (~1.9 ka) that erupted from the southwest foot of MSH is mineralogically and chemically distinct from the more evolved olivine basalt/basaltic andesite lava flows and scoria that erupted later (~1.7-1.6 ka) from summit vents.

Mineral Assemblages in the Tephras

Distinctive mineral assemblages characterize the tephras of each eruptive stage, from the earliest to the present; here we use the progression of these assemblages to help trace temporal variations of the MSH magmas. This entails two simplifications: (1) the assumption that crystal assemblages in the tephras give a reasonable indication of magma composition, and (2) the assumption that tephras alone (*i.e.*, without temporally associated lavas) give a meaningful indication of magma compositional trends at MSH. These assumptions are now briefly examined.

(1) Microprobe compositions of the tephra glasses are needed to accurately assess melt compositions. At present, however, such data are available for only some of the many tephra layers (Smith, 1984; Smith and Leeman, 1987). Also, weathering has changed the compositions of some of the older tephra glasses (Smith and Leeman, 1987; Melson, unpublished data). In contrast, tephra mineral assemblages are completely represented, layer by layer, from the earliest tephras to the latest (Mullineaux, 1986)(Figure 2), and these remain unaffected by glass alteration. The tephra mineral assemblages, like phenocrysts in lavas, represent (in most cases) minerals that were crystallizing from their magmas at near-liquidus temperatures, thus providing a guide to magma composition. Clearly, liquidus phases depend also on P, P_{H_2O}, f_{O_2}, *etc.* However, the correlation of phenocryst assemblages with volcanic rock composition (SiO_2), based on the chart shown in Figure 3, provides a rough empirical guide that works reasonably well for basalts to dacites in the Cascade Range. Plagioclase is ubiquitous and sanidine absent in all MSH rocks and tephras; therefore the Fe-Mg minerals and in some cases quartz are the diagnostic minerals.

(2) By looking at ***tephras alone***, we are missing the important contribution that lavas (in lava flows, domes, and lithic pyroclastic flows) make to the overall record of magma compositional variation with time. Eruptions at MSH typically begin, after a repose interval, with tephra-producing pyroclastic eruptions, followed by lava emission (domes or flows). It is desirable to trace the compositional progression of the full eruptive sequence, including the lavas as well as the tephras, but that is generally not possible except for the youngest eruptives (Spirit Lake stage). The domes and lava flows rarely extend far from the vent area and they have mostly been buried beneath the younger eruptives. However, the more distal tephras remain exposed and reasonably well preserved, and the tephra sequence back to about 40 ka has been documented in exceptional detail by D.R. Mullineaux (1986)(see Figure 2). Thus, in principle, it should be possible to follow compositional variation of the tephra-producing magmas through time, recognizing that the intervening compositional fluctuations produced by the lavas are lost.

Long-term compositional trend of MSH magmas. The MSH tephras show an ***overall*** progression of Fe-Mg mineral assemblages from bi+cm+hb (~40-36 ka), to cm+hb±hy (21-18 ka, 13-11 ka, 4-3 ka), to hb+hy±ag and hy-ag (3-1.7 ka, 1.2-0.2 ka) [ol=olivine; ag=augite; hy=hypersthene; hb=hornblende; cm=cummingtonite; bi=biotite; pl=plagioclase; qz=quartz]. Also, quartz is present in pyroclastic flows associated with only the earliest tephras (Figure 4). This mineralogical succession represents a progression of magma compositions from rhyodacite through dacite to andesite. We suggest that this progression, erupted over the relatively brief time span of about 40,000 years, represents the progressive tapping of a crystallizing magma body that possessed a vertical compositional gradient from H_2O-rich rhyodacite downward to less hydrous andesitic magma at depth. This suggestion is based on a comparison with silicic magma systems that have erupted zoned ignimbrites, inferred to have come from magma reservoirs that had developed vertical compositional and thermal gradients over time spans of up to 10^6 years (Smith, 1979; Hildreth, 1981; Grunder and Mahood, 1988).

An obvious difference between compositionally zoned ignimbrites and the MSH eruptive sequence is that the former disgorged the zoned upper portions of their magma chambers in single, large-volume caldera-forming eruptions, whereas MSH bled off the upper part of its underlying magma body in numerous small batches spaced over ~40,000 years. Greater depth of the MSH magma body (see below) may have been one factor in this different behavior. Moreover, it might be expected that the MSH magma system ***continued to evolve***, rather than remaining static, during its 40,000-year eruptive span. This evidently was the case, as indicated by: (1) its cyclic eruption pattern, including cyclic compositional variation, and (2) its dilution by basaltic magma at about 2.5-1.6 ka.

Cyclic composition trends of MSH magmas. A cyclic eruption pattern is superimposed on the long term (overall) compositional trend described above. This encompasses first-order, second-order, and third-order cyclicity. ***First-order cycles*** (10^3-10^4 years) consisted of eruptive intervals (stages) lasting about 2,000-4,000 years separated by dormant intervals of about 6,000-7,000 (possibly up to 15,000?) years (Figure 4). ***Second-order cycles*** (10^2-10^3 years) are represented by eruptive periods separated by repose intervals ***within*** each eruptive stage. Such second-order cycles are clear only within the most recent (*i.e.*, Spirit Lake) eruptive stage (Figures 4 and 5), but indications suggest that similar cyclicity also occurred within earlier stages (Mullineaux, 1986; see also Figure 4). ***Third-order cycles*** (months, years, tens of years) comprise the pattern of pyroclastic eruptions followed directly by lava emission followed by a repose interval, this sequence recurring repeatedly within a single eruptive period. Such short-term eruptive cycles were directly observed at MSH during 1980-82 (Melson, 1983), and are readily inferred from the stratigraphic evidence of alternating pyroclastic deposits and lavas throughout the Kalama eruptive period (Hopson and Melson, 1984; see also below).

First-order eruption cycles at MSH typically progressed from cm+hb(±bi) rhyodacite or dacite to hy+hb(±cm) or hy+hb±ag dacite (or siliceous andesite) tephra (Figures 2 and 4). Second-order cycles within eruptive stages perhaps show this trend better (see Figures 2 and 4: tephra sets C, M, J, Y+P, W+X). The ***mineralogic*** trend from amphiboles to pyroxene(s) in the tephras of individual eruption cycles points to a decrease in water content of the melt as the cycle progressed. The ***bulk composition*** trend toward less silicic magma as each cycle progressed suggests that each eruption cycle tapped a magma body that was compositionally and thermally zoned. The ***repetition*** of such cycles, separated by repose periods, indicates that the compositional and thermal gradients were restored toward the top of the magma body during the repose period.

The tephra sequences alone, however, convey an incomplete picture. We now turn to young eruption cycles at modern Mount St. Helens where other eruptive products can also be identified.

Eruption Cycles at Mount St. Helens within the last 4,000 years

Eruptions within about the last 4,000 years at MSH (Spirit Lake eruptive stage) typically come in eruption cycles that consist of a repose interval followed by a shorter eruption interval in which the character of the eruptions progressed from Plinian eruptions that deposited pumiceous tephra to lava dome building with diminished pyroclastic activity, lithic (non-pumiceous) pyroclastic flows and lesser tephras, to (lastly) eruption of lava flows alternating with pyroclastic outbursts that left small-volume scoria and ash deposits. The succession of pyroclastic rocks and lavas during each eruptive interval show a chemical progression from silicic to

ERUPT. STAGE	ERUPT. PERIOD	TEPHRA SET	TEPHRA LAYER	MAGMA COMP.	OL	AG	HY	HB	CM	BI	LAYER AGES
SPIRIT LAKE	Goat Rx	T	T	D		●	●	●			AD 1800
	Kalama		z	D		●	●	●			
		X	Xh	A	●	●	●				
			Xm	A	●	●	◉				
			Xs	A	●	●	●	●			
			Xb	A	●	●	●	◉			
		W	Wd	D			●	●			
			We	D			●	◉			AD 1482
			Wb	D			●	●			
			Wa	D			●	◉			
			Wn	D			●	●			AD 1480
	Sugar Bowl		D	D			●	●			1,200
	Castle Creek	B	Bu	B	●						1,620; 1,780
			Bi	D		●	●				1,850
			Bd	D		◉	●	◉			2,060; 2,220
			bag	A							
			Bo	bA	●	●	●				
			Bh	A		●	●				
	Pine Creek	P	Py	D			●	●			2,450
			Pu	D			●	●			
			Ps	D			●	●			
			Pm	D			●	●			
	Smith Creek	Y	Yu	D				●	●		2,930
			Yo, Yf (yp)					●	●		
			ya (yc)					●	●		3,350
			Ye (yc)	D				●	●		
			Yn	D				●	●		3,510
			Yd	D				●	●		
			Yb	RD?				●	●	◉	
											3,900; 9,170
SWIFT CREEK		J	Jg	A		◉	◉	●			10,710
			Jb	A			●	●			
			Jy	D			●	●			
			Js	D			●	●			
											11,500; 11,700; 12,120
		S	So	D			◉	●	●		
			Sg	D			◉	●	●		
			Ss	D			◉	●	●		12,910
			Sw	D				●	●		
			Sb	D			◉	●	●		
											13,650; 19,160
COUGAR		K	K					●	●		
		M	Mt	(D)			●	●			
			Mm	(D)			●	●			
			Mp	(D)			●	●	●		
			Mc	(D)			◉	●	●		
			Mo	(D)	○		◉	●	●		
			Mg	(D)				●	●		
			ms	(D)				●	●		20,350
	At least four obscure, unnamed groups of cummingtonite-bearing tephras, pyro.flows & ashy seds.								○ ○ ○ ○		
APE CANYON		C	Cs	RD				●	●	◉	
			Cy	RD				●	●	◉	
			Cm	RD				●	●	◉	36,000
			Cw	RD				●	●	◉	
			Ct	RD			◉	●	●	◉	37,600
			Cb	RD				●	◉	◉	

Figure 2 *Mount St. Helens tephra units, compositions, and ages. Tephra sets, tephra layers, and eruptive stages and periods are shown in the left-hand columns. Inferred bulk compositions of the tephras (=magmas) are:* ***RD****, rhyodacite;* ***D****, dacite;* ***A****, andesite;* ***bA****, basaltic andesite;* ***B****, basalt. Fe-Mg minerals within the tephras are:* ***OL****, olivine;* ***AG****, augite;* ***HY****, hypersthene;* ***HB****, hornblende;* ***CM****, cummingtonite;* ***BI****, biotite. Filled circles represent major minerals; circles with dots are subordinate minerals; open circles are minor minerals. Right-hand column shows stratigraphic position and ages of layers (both tephra and other) dated by radiocarbon method and by tree ring counts. Radiocarbon ages are in years before 1980; tree-ring ages are in years A.D. Data taken from Mullineaux (1986, table 1); bulk composition estimates modified by Hopson.*

more mafic bulk compositions and a mineralogical progression in which phenocrystic hornblende diminished and then disappeared while augite and then olivine appeared and then increased. Eruption cycles showing this trend are the Smith Creek-Pine Creek-early Castle Creek cycle, the Kalama cycle, and the Goat Rocks cycle, which are of progressively diminishing volume and duration. In addition, arrested eruption cycles consisting of small-volume tephra eruptions followed by minor dome growth occurred three times: the Dogs Head event, the East Dome event, and the Sugar Bowl event. The pattern of cyclic eruptions was interrupted when basaltic magma entered the MSH magma system during the Castle Creek eruptive period.

Smith Creek-Pine Creek-early Castle Creek eruption cycle. The Spirit Lake eruptive stage, following a 7,000-year dormant interval, began with a prolonged eruptive progression that encompassed the Smith Creek and Pine Creek eruptive periods and earliest part of the Castle Creek period (Figure 1). The 7,000-year dormant interval and subsequent eruptive interval (lasting at least 1,200 years; see Figure 5) comprise the Smith Creek-Pine Creek-early Castle Creek eruption cycle. The eruptive part of this cycle began with Plinian and sub-Plinian eruptions that produced voluminous pumiceous tephras (Set Y, Figure 2) interspersed with the eruption of pumiceous and lithic pyroclastic flows and lahars (Crandell, 1987). Pyroclastic flows with nonvesicular (lithic) clasts record the growth of lava domes (possibly ephemeral) during this initial period (Smith Creek). The cycle then progressed to a mainly dome-building period (Pine Creek), characterized by the growth of a cluster of lava domes over the vent area and voluminous, dominantly lithic pyroclastic flows and lahars moving down the adjacent stream valleys (Crandell, 1987). Dome remnants of probable Pine Creek age are exposed in the east, south, and west walls of the MSH 1980 crater and also crop out on the west and southwest flanks of the mountain (Hopson and Melson, 1982; Hopson, unpublished map). Four major tephra layers (Set P), in addition to voluminous ash-cloud deposits on the southeast side of MSH, resulted from recurring large pyroclastic eruptions. However (quoting Crandell, 1987, p. 52), "Pine Creek time was characterized by the eruption of small volumes of tephra and the formation of many pyroclastic flows, in contrast to the [preceding] Smith Creek eruptive period when much larger volumes of pumiceous tephra were erupted but fewer pyroclastic flows occurred". The third and last stage of the eruptive cycle entailed the voluminous outpouring of andesitic lavas accompanied by minor pyroclastic products (tephra layers Bh, Bo, and possibly bag and bab; see Figures 2 and 5 and Table 1). These include the most voluminous and far-reaching andesitic lava flows found at MSH. Remnants of their distal parts were mapped before 1980 at Muddy River (8 km from MSH), Kalama Spring (8 km), Castle Creek (up to 10 km), lower west fork of Wishbone Glacier Creek (6.5 km), and at several closer locations on the N-NNE flanks of the mountain (Hopson, unpublished map). An olivine-bearing andesitic tephra (Bo layer) marks the end of this eruption cycle. Corresponding lava flows have not yet been identified but may be among the flows collectively mapped as the Timberline Basalt unit (Hopson, unpublished map). In summary, following a long repose interval, this eruption cycle progressed from highly explosive, chiefly pyroclastic eruptions to dome building and lithic pyroclastic flows to the outflow of fluid magma as lava flows. A progressive decrease in volatile content of the magma seems indicated.

The tephras of the Smith Creek-Pine Creek-early Castle Creek eruption cycle show a remarkable time progression of Fe-Mg mineral assemblages: bi-cm-hb, cm-hb, hb-hy, hy-ag, ol-hy-ag (Figure 5). This, too, reflects a progressive decrease in magma H_2O content from that close to H_2O saturation (indicated by cummingtonite, see below) to increasingly more undersaturated magma. The progressive tapping of a magma body that had a strong vertical gradient of H_2O seems indicated. Moreover, the Fe-Mg mineral assemblages in the tephra sequence point to a progression in magma composition from rhyodacite or siliceous dacite to andesite (compare Figures 3 and 5). A progression from dacite to andesite (SiO_2 = 66.5% to ~58%) is also documented by available whole-rock chemical analyses of pumices and rocks from these periods (Smith and Leeman, 1987, table 5; Melson, unpublished analyses). Thus, we infer that this eruption cycle represents the progressive tapping of a magma body that possessed a vertical gradient from rhyodacitic to andesitic magma, developed during the preceding 7,000 years.

Kalama eruption cycle. The Kalama cycle, comprising a 700-year repose period followed by the Kalama eruptive period (A.D. 1480 to A.D. 1600±30; see Figure 1), shows a similar eruptive pattern and compositional variation. The eruptive period progressed through the following steps, determined from geologic mapping and stratigraphy (Hopson and Melson, 1984; in prep.): (1) Plinian eruptions in A.D. 1480 and A.D. 1482 (Yamaguchi, 1985) produced voluminous, far-reaching pumice deposits (Wn, We tephra layers of Mullineaux, 1986), leaving a closed summit crater >500 m deep; (2) early dome growth within the crater was accompanied by pyroclastic eruptions that sent dacitic lithic pyroclastic flows down the Kalama River valley through a breach in the SW crater wall; also, a sub-Plinian eruption deposited pumiceous tephra on MSH north flank and a pumiceous lahar in Kalama River valley; (3) continued growth of an endogenous dome within the closed crater; dome lava finally overtopped the crater rim sending a dacitic pyroclastic flow down the northwest flank of MSH into Castle Creek, followed later by a hot block avalanche down the west flank; (4) eruption of copious andesitic magma from vents around the dome margin, sending lava flows down most sides of the mountain (especially voluminous on the south); ***pyroclastic outbursts*** alternated with ***lava emission*** during this stage, producing scoria and ash beds interstratified with thin lava streams close to the vent (exposed in the MSH 1980 crater wall) and pyroclastic flows that were overridden by co-eruptive lava flows (pyroclastic flow-lava flow couplets) on the lower flanks of

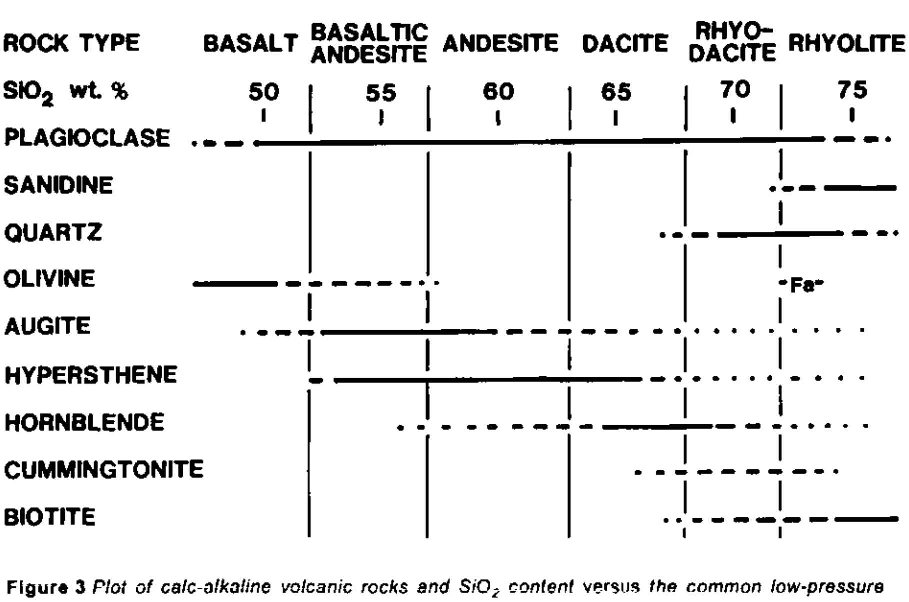

Figure 3 *Plot of calc-alkaline volcanic rocks and SiO_2 content versus the common low-pressure phenocrystic minerals. Solid lines depict the common range of phenocryst types; dashed and dotted lines show the extended distribution range under restricted range of T, P_{H_2O}, or f_{O_2}. Plot is constructed from mineralogical and chemical data for young volcanic rocks of the Cascade Range, northwestern US.*

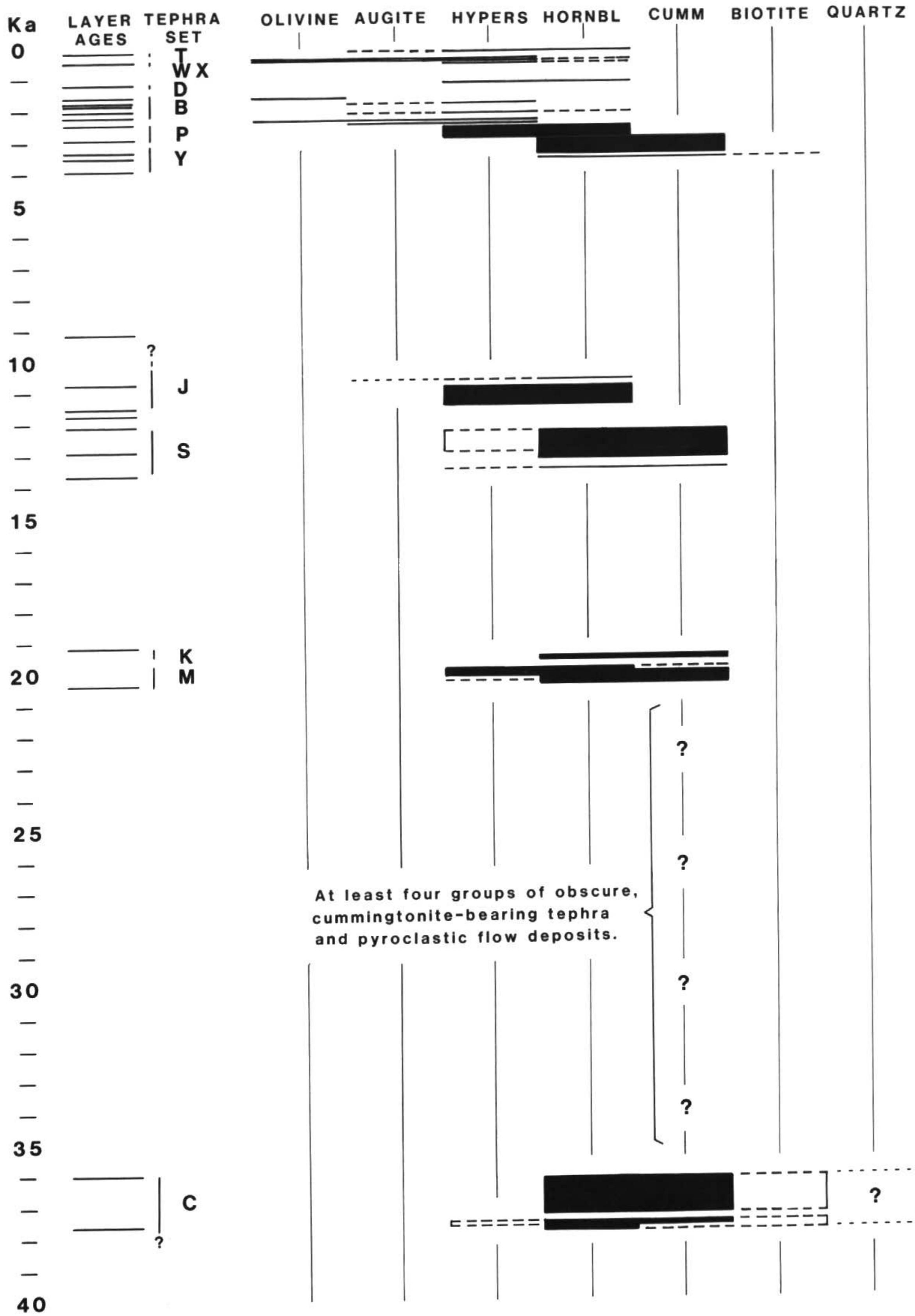

Figure 4 *Fe-Mg mineral assemblages for Mount St. Helens tephras, spanning the lifetime of the volcanic center before 1980. Time scale in thousands of years (ka). The ages of dated layers (radiocarbon or tree ring ages), which constrain the ages of the tephra sets and layers, are shown for comparison. Solid lines and blocks depict major minerals, dashed lines and blocks the subordinate minerals, and dotted lines and blocks the minor minerals. Data from Mullineaux (1986). Presence or absence of quartz in the tephras has not been recorded; quartz phenocrysts are found in pyroclastic flows of Ape Canyon (C tephra) age, but not in younger flows.*

the volcano; (5) eruption of basaltic andesite producing a pyroclastic flow/lava flow couplet (MSH south flank); (6) resurgence of the thick (>500 m) endogenous dome that was still cooling within the closed crater, causing upheaval above the crater rim and avalanching of blocks and ash down the southeast, south, southwest, and northwest flanks of the mountain. These avalanches (or debris flows) comprised a unique mixture of hot dacite from the dome interior and cold, in part fumarolically altered, dacite from the dome carapace and blocks of dark lava from the coronet of andesitic cones that had encircled and mantled the dome. In summary, the Kalama eruptive cycle progressed from explosive pyroclastic eruptions to dome growth with pyroclastic flows to the outflow of voluminous lava. This resembles the earlier, more voluminous Smith Creek-Pine Creek-early Castle Creek eruption cycle. The better-preserved Kalama deposits, however, show also that pyroclastic outbursts (producing tephra and pyroclastic flows) alternated with lava emission (as dome increments and lava flows) on a short time scale throughout the eruption cycle. We infer that the Kalama magma body had developed a strong vertical H_2O gradient by the time the eruption cycle began, but that H_2O was ***repeatedly replenished*** toward the top of the magma chamber during the ensuing 100-150 years of eruptive activity.

The Fe-Mg phenocrystic minerals in rocks and tephras of the Kalama period show the following progression with time, corresponding to the eruption steps described above: (1) hy>hb; (2) hy>>hb; (3a) hy>ag>hb; (3b) hy>ag>>hb; (4) ag=hy (4a contains opacitic hornblende relics; 4c contains minor resorbed olivine); (5) ag>hy>ol; (6) hy>hb=ag; see Figure 6. The summit dome dacites are assigned to step 6 based on the stratigraphic position of their avalanche/debris flow deposits on the flanks of the volcano, but the dacite itself was ***erupted earlier***, between steps 2-3, when the dome was growing within the closed crater. Thus, with this adjustment, it is seen that there was a steady decrease and then disappearance of hornblende, and progressive increase in augite and then olivine (Figure 6). We infer a progressive decrease in H_2O content of the melt as well as a progressive change in magma composition.

Figure 7, a plot of SiO_2 *versus* time (shown as eruption steps) for 62 analyzed rocks of the Kalama period, reveals progressive decrease in SiO_2 for steps 1 through 5, followed by an abrupt apparent reversal for the summit dome rocks of step 6. When the summit dome compositions are shifted back to the time gap between eruption steps 2 and 3, when the dome is inferred to have grown while enclosed within a large summit crater, there is a consistent progression with time toward increasingly more mafic compositions throughout the Kalama period.

We interpret this compositional/temporal progression as the product of successive

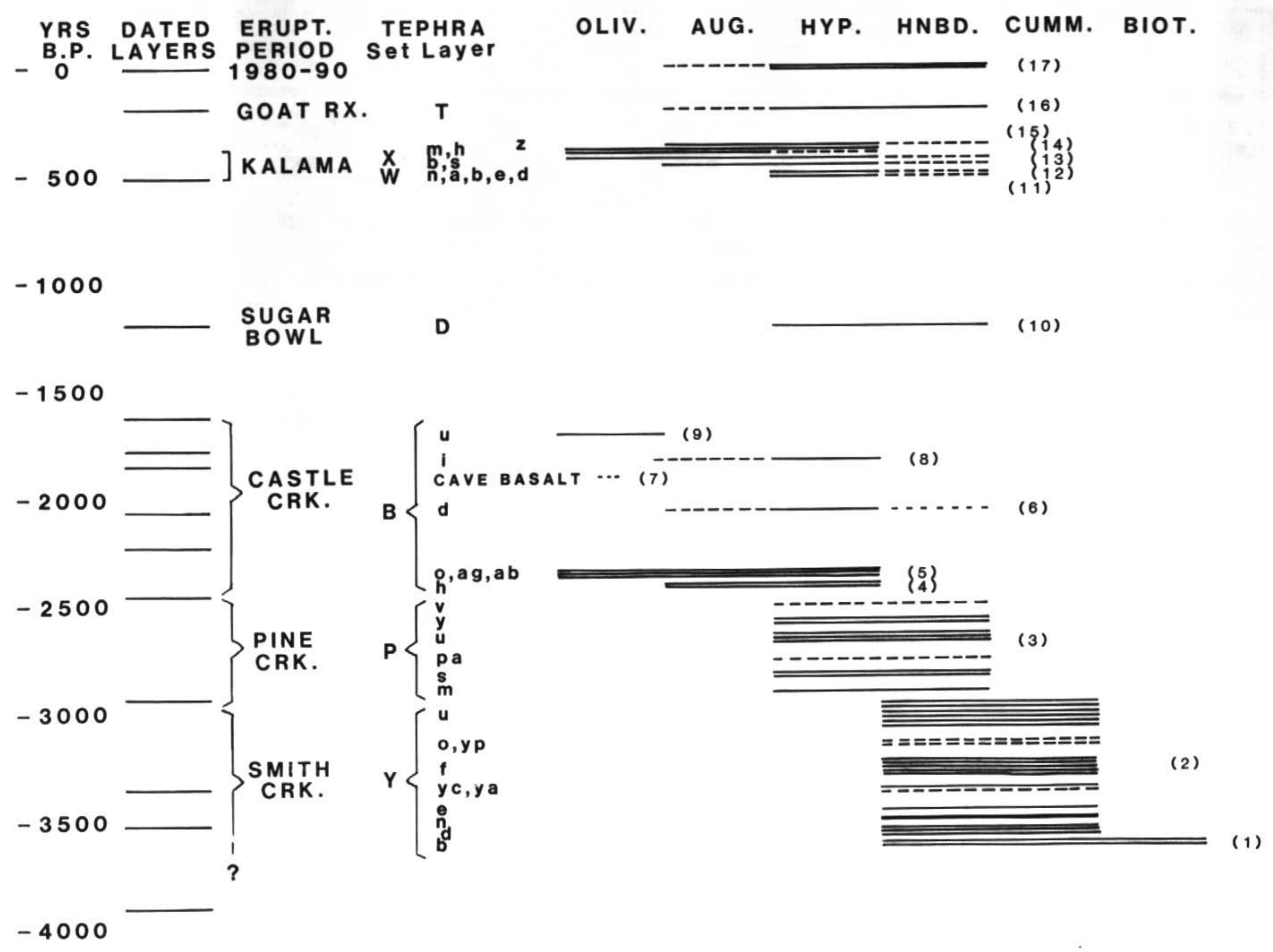

Figure 5 *Fe-Mg mineral assemblages for Mount St. Helens tephras of the Spirit Lake eruptive stage. Time scale in years before 1980. Dated layers that constrain the age of the tephras are shown for comparison; ages in radiocarbon years. Fe-Mg mineral assemblage shown for each tephra layer. Solid lines depict major minerals, dashed lines for subordinate minerals, dotted lines for minor minerals. Data from Mullineaux (1986). Numbers in parentheses opposite tephra layers or sets correspond to the numbers in Table 1, which identify pyroclastic flows, lava flows and domes that are correlated (by Hopson) with these tephras.*

eruptions that tapped progressively deeper levels of a magma body that had vertical gradients in magma composition, H_2O content and temperature. Temperature ranged from 840°C at the top of the magma column to 1000±20°C at the deepest level tapped, as determined by magnetite-ilmenite thermometry for pumice of layers Wn, We (Smith and Leeman, 1987) and for basaltic andesite of step 5 (Rutherford and Devine, 1989). These gradients developed during the 1,100-year interval of inactivity that followed the Castle Creek eruptive period. The brief Sugar Bowl pyroclastic surge and dome-building event (hb-hy dacite) at 1.15 ka probably did little to interrupt the re-establishment of compositional and thermal gradients during the 1.6 ka to 0.51 ka repose period.

Goat Rocks eruption cycle. The Goat Rocks eruptive period (A.D. 1800 to A.D. 1857) followed only about 200 years of repose. It comprises the following eruptive events: (1) Plinian eruption of dacite pumice (tephra layer T; hy>hb>ag; SiO_2 = 65.2-63.1%) from a vent on the northwest flank of MSH; (2) growth of a dacite lava dome (hy>ag>hb; SiO_2 = 63.7-62.4%) at this vent; (3) extrusion of andesitic lava (ag=hy >> hb; SiO_2 = 62.7-60.2%) at the base of the dome, forming a lava flow 4.6 km long (Floating Island flow); and (4) resurgence (upheaval) of the dome, resulting in avalanche/debris flows of mixed hot blocks (radially jointed) and cold blocks (no jointing; some with fumarolic alteration) between pulses of andesite extrusion (Hopson and Melson, 1984). The first three events produced successive magmatic products of the Goat Rocks eruption cycle. The fourth event produced no new magmatic rock (but note the different interpretation of Hoblitt *et al.* (1980), Mullineaux and Crandell (1981), and Crandell (1987)).

Thus, the Goat Rocks cycle mirrors the pattern of previous eruption cycles, but the products are less fractionated, much less voluminous, and the cycle was of shorter duration. This reflects the much shorter repose period and thus the lesser extent to which magma chamber gradients could recover.

Basalt. Olivine basalt (SiO_2 = 49.5-50.2%; K_2O = 0.41-0.52%) erupted from the southwest base of MSH at ~1.9 ka forming voluminous lava flows in the Kalama River and Swift Creek-Lewis River drainages (Cave Basalt of Greeley and Hyde, 1972). Later, olivine basalt and basaltic andesite (SiO_2 = 51.2-56.1%; K_2O = 0.90-1.06%) erupted from vents near the summit of MSH between 1.78-1.62 ka, forming voluminous scoriaceous tephra (Bu layer is the distal fringe) and sending lava flows down the northwest, north, northeast, and south flanks of MSH. Before these events, the appearance of olivine-bearing basaltic andesite tephra (Bo layer of Mullineaux, 1986) between 2.45-2.22 ka may indicate that basaltic magma had already entered the MSH magma system. Halliday *et al.* (1983) conclude from geochemical and isotopic evidence that mantle-

Table 1 Correlation of pyroclastic flows, lava flows and domes with tephras of the Spirit Lake eruptive stage.

Tephra units	Related pyroclastic flows, lava flows & domes
(1) Layer Yb	None recognized
(2) Set Y except Yb	Pumiceous and lithic dacitic pyroclastic flows. Dome remnant (Smith Crk?) at base of NW crater wall, MSH
(3) Set P all layers	Voluminous lithic hb-hy dacite pyroclastic flows in stream valleys from MSH. Dome remnants in E,S,W craters walls and on W and SW flanks, MSH
(4) Layer Bh	Hy-ag andesite lava flow remnants (distal) at Muddy River, Kalama Spring, and, before May 1980, at Castle Creek, lower west fork Wishbone Glacier Creek, and several locations on the N-NNE flank of MSH
(5) Layers Bo, Bag, Bab	Tephra only? Alternatively, some basalt-basaltic andesite lava flows now mapped as Timberline Basalt (1.6-1.7 ka), but poorly constrained stratigraphically, may instead be older flows related to these tephras
(6) Layer Bd	Dogs Head dome (hb-ag-*hy* dacite), NNE flank of MSH
(7) No tephra?	Cave Basalt (1.9 ka) of Kalama River and Lewis River valleys
(8) Layer Bi	East Dome, lower E flank of MSH. Distinctive hy dacite (+ minor ag, hb), unique at MSH, comprises both the dome lava and the Bi pumice
(9) Layer Bu	Timberline Basalt: includes lava flows of olivine basalt and basaltic andesite on the NE, N, NW, SW and S flanks of MSH as well as lava flows and associated reddish scoria layers in MSH 1980 crater wall
(10) Layer D	Sugar Bowl dome (hb-hy dacite) on N flank of MSH
(11) Layers Wn, Wa, Wb, We	No associated lava. Plinian eruptions left a large closed crater 500 m deep
(12) Layer Wd	Pyroclastic flows (several lithic and one pumiceous) of hb-hy dacite, Kalama River valley
(13) Layers Xb, Xs	Summit dome of hb-ag-hy dacite, growing inside the closed crater of MSH, and a pyroclastic flow (Castle Creek) and a block/ash avalanche (W flank MSH) where growing dome overtopped crater rim. [Olivine in Xb, Xs tephras is a contaminant from earlier Bu scorias that repeatedly blocked the MSH vent]
(14) Layers Xm, Xh	Lava flows and pyroclastic flow/lava flow couplets of hy-ag andesite on flanks of MSH (most sides), and an ol-hy-ag andesite pyroclastic flow /lava flow couplet on S flank of MSH
(15) Layer z	Resurgence (upheaval) of MSH summit dome from closed crater, with avalanching of mixed cold blocks (from dome carapace) and hot blocks (from dome interior) and ash down the W, SW, S, and SE flanks of MSH
(16) Layer T	Goat Rocks dome (ag-hb-hy dacite) on NNW flank of MSH
(17) 1980-83 tephras	Lava dome (ag-hb-hy dacite) in MSH 1980 crater

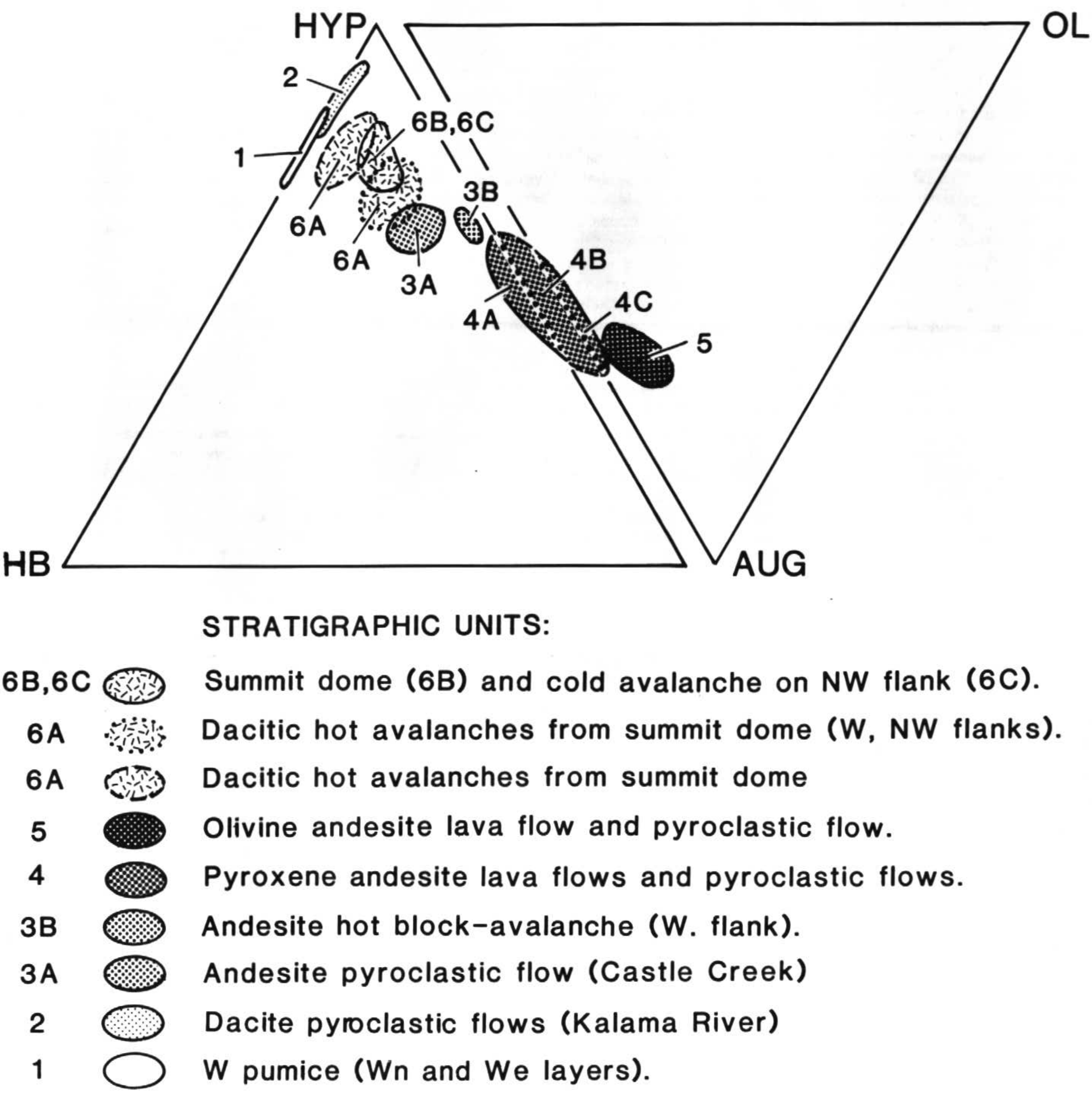

Figure 6 *Modal plots for hornblende-hypersthene-augite and hypersthene-augite-olivine showing the Fe-Mg (micro)phenocryst assemblages for rocks and tephras of the Kalama eruptive period. Rock units arranged in stratigraphic order from lowest (=1) to highest (=6). Fields for each unit determined by visual estimation of mineral proportions in thin section. Units 6A, 6C (avalanche/debris-flow deposits of summit-dome lavas) overlie units 1-5 on the flanks of MSH but the dome rocks formed earlier (between 2-4) within a closed crater. See text for discussion.*

derived basaltic magma entered the MSH magma reservoir, contaminating and modifying MSH magma which had, until that time, a more crustal isotopic signature.

Discussion

The cyclic eruptions and, to some extent, the long-term trend at MSH reveal a similar pattern: (1) an eruptive progression from highly explosive eruptions to dome building with progressively less explosive eruptions to (in some cases) fluid lava emission punctuated by small explosive outbursts; (2) a mineralogic progression from hydrous Fe-Mg phenocrysts (bi, cm, hb) toward anhydrous equivalents (hy, ag); and (3) a magmatic compositional progression from more silicic (rhyodacite or dacite) toward less silicic (andesite or basaltic andesite) compositions, reflecting progression from moderately fractionated to less fractionated magma. The fact that the long-term trend follows roughly the same patterns as the shorter cyclic patterns suggests that similar magmatic controls apply to both.

Rise of volatiles, especially H_2O, concentrating toward the top of the magma reservoir during repose periods, is an important control for both the eruptive and mineralogic progressions. This process has been directly demonstrated in connection with cyclic eruptions on a very short time scale during the 1980-82 eruptions at MSH. These cycles followed the pattern: (1) repose interval (months), (2) pyroclastic eruption (minutes or hours), (3) lava dome growth (days, weeks). A systematic decrease in water content of the melt (as demonstrated by glass inclusion studies of Melson, 1983) from pyroclasts to lava is apparent in most of these eruption couplets, followed by replenishment of H_2O during the intervening repose periods (see fig. 2 in Melson, 1983). Volatiles evidently migrated continuously toward the top of the magma column, establishing a vertical gradient of volatiles within the magma. Eruptions behead this gradient, but volatile migration upward during ensuing repose periods works toward its renewal.

The ***mineralogic*** progressions during the MSH cyclic eruptions (Figures 5 and 6) also demonstrate the existence of H_2O gradients, and the repetition of the mineralogic progressions in subsequent cycles show that H_2O gradients were re-established during repose periods. Information from amphiboles is especially informative. H_2O contents of at least 6% (at 4 kb) are necessary to crystallize hornblende early (*i.e.*, as phenocrysts) in melts of dacitic to andesitic composition, whereas pyroxene crystallizes instead at lower H_2O contents (Merzbacher and Eggler, 1984). The occurrence at MSH of cummingtonite, which takes the place of hypersthene in siliceous melts at high H_2O contents, is especially interesting. Cummingtonite phenocrysts in Taupo (NZ) rhyolites crystallized from magma that contained 9-12% H_2O under conditions of P_{H_2O} at or near P_{total} (Wood and Carmichael, 1973). Calculations by these authors show that $P_{H_2O} > 0.7\text{-}0.8\ P_{total}$ are necessary for cummingtonite to crystallize in rhyolites (note that cm-bearing tephra at MSH have rhyolitic glass; see Smith and Leeman, 1987). Moreover, fairly high P_{total} (>5 kb?) is also needed for cummingtonite to crystallize early from these melts (Wood and Carmichael, 1973). In light of these observations, the mineralogic progression from cm+hb, to cm+hb+hy, to hb+hy in MSH eruptive sequences (Figures 4 and 5) probably reflects the progressive

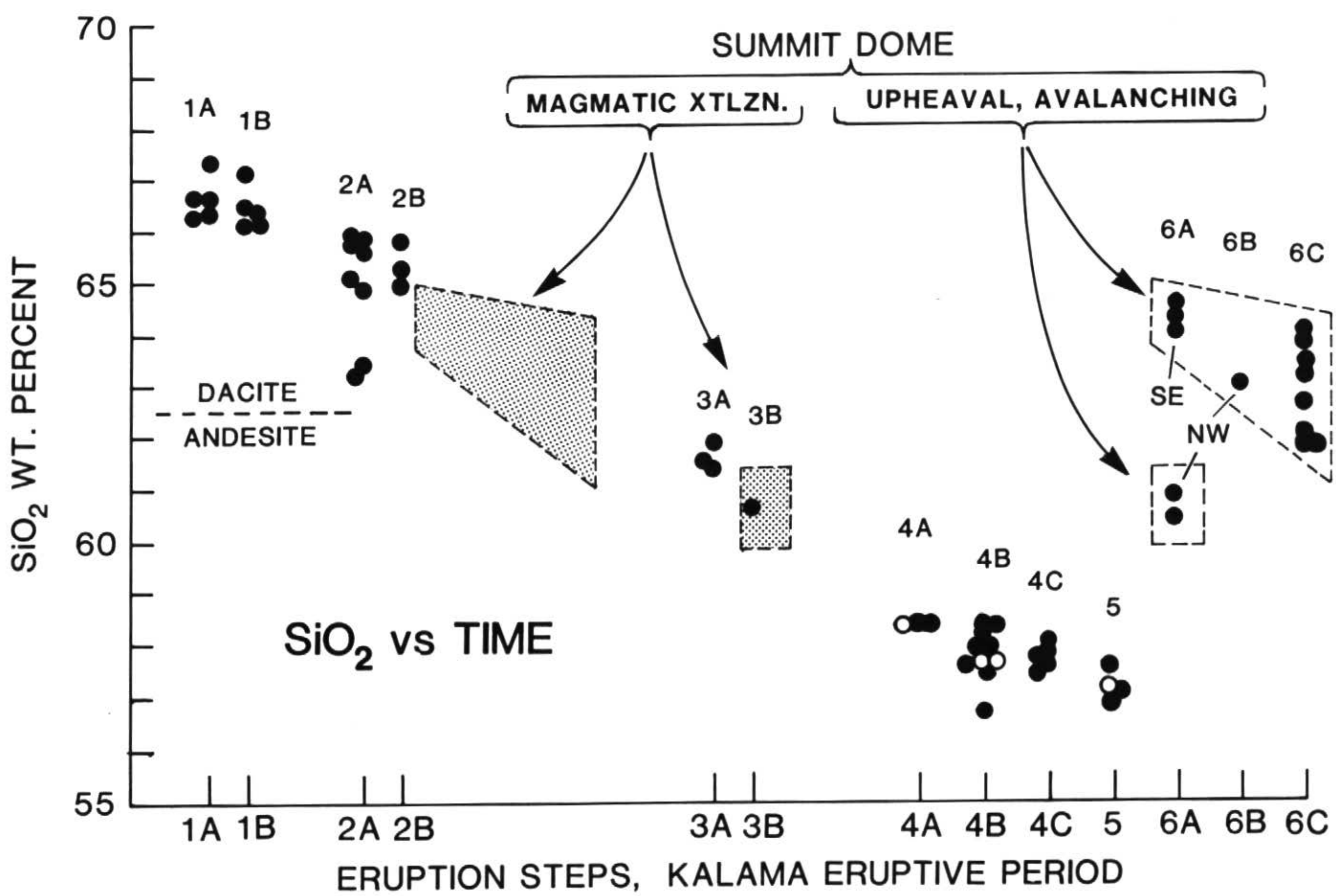

Figure 7 *Plot of SiO_2 versus time (shown as eruption steps) for 62 analyzed rocks and pumices of the Kalama eruptive period. Eruption steps are those described in the text. **1A**, Wn pumice; **1B**, We pumice; **2A**, lithic clasts in Kalama River pyroclastic flows; **2B**, air-fall (MSH N flank) and lahar (Kalama River) pumice; **3A**, clasts in Castle Creek pyroclastic flow; **3B**, clast in hot block flow (MSH W flank); **4A**, hornblende-bearing pyroxene andesites; **4B**, pyroxene andesites; **4C**, olivine-bearing pyroxene andesites; filled circles are lavas and open circles are pyroclastic flows; **5**, olivine-pyroxene andesites; **6A,6B**, summit dome lava in avalanche deposits on SE and NW flanks of MSH; **6C**, summit dome lava in place.*

tapping of a deep magma body with pronounced H_2O gradients, approaching saturation toward the top.

The magmatic ***compositional*** progression that characterizes MSH cyclic eruption patterns (*e.g.*, Figure 7) indicates to us that compositional gradients are also developed toward the apex of the magma body during repose periods. Eruption beheads these gradients, but they are regenerated during repose periods. The discussion of specific fractionation processes is beyond the scope of this paper; however, some form of liquid fractionation may be important in the development of compositional gradients here as it is in some rhyolitic magmas (Hildreth, 1979, 1981; Mahood, 1981). Smith and Leeman (1987) show that fractional crystallization alone is not a viable control.

Conclusions

Mount St. Helens shows cyclic eruption patterns. Eruption cycles consisted of a repose interval in which compositional and thermal gradients developed within the upper part of the underlying magma body, followed by an eruption interval in which progressive tapping of the underlying magma reservoir beheaded part of its graded upper portion. Gradients were re-established during the ensuing repose period, the extent of recovery depending upon the length of the repose period. The products disgorged during an eruption interval follow the pattern: (a) an ***eruptive progression*** from Plinian eruptions that produced pumiceous tephra to lava-dome building accompanied by explosive eruptions that produced lithic pyroclastic flows and lesser tephra, followed (in some cases) by lava flows punctuated by small pyroclastic eruptions; (b) a ***mineralogic progression*** from hydrous Fe-Mg phenocrysts (hb, cm, bi) toward anhydrous equivalents (hy, ag); and (c) a ***magmatic compositional progression*** from more silicic (rhyodacite or dacite) toward less silicic (andesite) magma. The eruptive and mineralogic progressions result mainly from vertical gradients of volatile content (especially H_2O) in the magma reservoir. The compositional progression and, to some extent, the mineralogical progression (especially bi, ol) reflect gradients of melt composition and crystal content.

First-order eruption cycles at MSH, only dimly perceived from the surviving tephra sequence, comprised eruption intervals (stages) lasting 2,000-4,000 years and dormant intervals lasting 5,000-7,000 (up to 15,000?) years. The eruption stages are overprinted and partly obscured by second-order cycles with eruption intervals (periods) lasting tens to hundreds of years separated by repose intervals typically lasting hundreds of years. Third-order eruption cycles, spanning only months, years, or tens of years, consisted of explosive eruptions followed directly by lava emission, followed (we infer) by a repose period. Volatile, but not compositional, gradients recovered during the brief repose periods.

The 40,000-year eruptive history of MSH reveals an overall compositional trend from rhyodacite to andesite, basaltic andesite and basalt. This may reflect the presence of a rising, crystallizing, vertically graded magma body (pluton) that periodically supplied magma to the surface. Eruption of basalt and hybrid andesite beginning ~2,500 years ago reflects entry of basaltic magma into the system.

Acknowledgements

We thank D.W. Peterson for critical review of the manuscript and for editorial assistance. CAH also acknowledges the invaluable support of the United States Geological Survey during field work at Mount St. Helens.

References

Crandell, D.R., 1987, Deposits of pre-1980 pyroclastic flows and lahars from Mount St. Helens volcano, Washington: United States Geological Survey, Professional Paper 1444, 91 p.

Crandell, D.R. and Mullineaux, D.R., 1978, Potential hazards from future eruptions of Mount St. Helens volcano, Washington: United States Geological Survey, Bulletin 1383-C, 26 p.

Crandell, D.R., Mullineaux, D.R. and Rubin, M., 1975, Mt. St. Helens volcano; recent and future behavior: Science, v. 187, p. 438-441.

Greeley, R. and Hyde, J.H., 1972, Lava tubes of the Cave Basalt: Geological Society of America, Bulletin, v. 83, p. 2397-2418.

Grunder, A.L. and Mahood, G.A., 1988, Physical and chemical models of zoned silicic magmas: The Loma Seca Tuff and Calabozos caldera, southern Andes: Journal of Petrology, v. 29, p. 831-867.

Halliday, A.N., Fallick, A.E., Dickin, A.P., Mackenzie, A.B., Stephens, W.E. and Hildreth, W., 1983, The isotopic and chemical evolution of Mount St. Helens: Earth and Planetary Science Letters, v. 63, p. 241-256.

Hildreth, W., 1979, The Bishop Tuff: Evidence for the origin of compositional zonation in silicic magma chambers: Geological Society of America, Special Paper 180, p. 43-75.

Hildreth, W., 1981, Gradients in silicic magma chambers: implications for lithospheric magmatism: Journal of Geophysical Research, v. 86, p. 10,153-10,192.

Hoblitt, R.P., Crandell, D.R. and Mullineaux, D.R., 1980, Mount St. Helens eruptive behavior during the past 1,500 yr: Geology, v. 8, p. 555-559.

Hopson, C.A. and Melson, W.G., 1982, Stratigraphy of the Mount St. Helens 1980 crater walls: EOS, v. 63, p. 1144.

Hopson, C.A. and Melson, W.G., 1984, Eruption cycles and plug-domes at Mount St. Helens: Geological Society of America, Abstracts with Programs, v. 16, no. 6, p. 544.

Mahood, G.A., 1981, Chemical evolution of a Pleistocene rhyolitic center: Sierra la Primavera, Jalisco, Mexico: Contributions to Mineralogy and Petrology, v. 77, p. 129-149.

Melson, W.G., 1983, Monitoring the 1980-1982 eruptions of Mount St. Helens: compositions and abundances of glass: Science, v. 221, p. 1387-1391.

Merzbacher, C. and Eggler, D.H., 1984, A magmatic geohygrometer: Application to Mount St. Helens and other dacitic magmas: Geology, v. 12, p. 587-590.

Mullineaux, D.R., 1986, Summary of pre-1980 tephra-fall deposits erupted from Mount St. Helens, Washington State, USA: Bulletin of Volcanology, v. 48, p. 17-26.

Mullineaux, D.R. and Crandell, D.R., 1981, The eruptive history of Mount St. Helens, *in* Lipman, P.W. and Mullineaux, D.R., eds., The 1980 eruptions of Mount St. Helens, Washington: United States Geological Survey, Professional Paper 1250, p. 3-15.

Rutherford, M.J. and Devine, J.D., 1989, Conditions in the Mount St. Helens magmatic system: Experiments on olivine-andesite: EOS, v. 70, p. 1394.

Smith, D.R., 1984, The petrology and geochemistry of High Cascade volcanics in southern Washington: Mount St. Helens volcano and the Indian Heaven basalt field, Ph.D. dissertation, Rice University, Houston, Texas, 409 p.

Smith, D.R. and Leeman, W.P., 1987, Petrogenesis of Mount St. Helens dacitic magmas: Journal of Geophysical Research, v. 92, p. 10,313-10,334.

Smith, R.L., 1979, Ash-flow magmatism, *in* Chapin, C.E. and Elston, W.E., eds., Ash-flow tuffs: Geological Society of America, Special Paper 180, p. 5-27.

Wood, B.J. and Carmichael, I.S.E., 1973, P_{total}, P_{H_2O} and the occurrence of cummingtonite in volcanic rocks: Contributions to Mineralogy and Petrology, v. 40, p. 149-158.

Yamaguchi, D.K., 1985, Tree-ring evidence for a two-year interval between recent prehistoric explosive eruptions of Mount St. Helens: Geology, v. 13, p. 554-557.